

Article

Properties of Diamond-like Tungsten-Doped Carbon Coatings Lubricated with Cutting Fluid

Krystyna Radoń-Kobus ^{*}, Monika Madej , Joanna Kowalczyk  and Katarzyna Piotrowska

Department of Mechatronics and Mechanical Engineering, Kielce University of Technology, Al. Tysiąclecia Państwa Polskiego 7, 25-314 Kielce, Poland; mmadej@tu.kielce.pl (M.M.); jkowalczyk@tu.kielce.pl (J.K.); kpawelec@tu.kielce.pl (K.P.)

* Correspondence: kradonkobus@tu.kielce.pl

Abstract: In this paper, the authors investigated the impact of DLC coatings doped with tungsten (a-C:H:W) coatings obtained using plasma-assisted physical vapor deposition (PVD) on the properties of the 100Cr6 steel. The results of the 100Cr6 steel specimens with and without the coating were compared. Scanning electron microscopy (SEM) and energy dispersive X-ray (EDX) analysis were used to observe the morphology of the coating surfaces and cross-sections and identify the elements in the coating composition. The contact angle of the investigated surfaces was measured with a tensiometer. Additionally, the effect of the coatings on the tribological properties of lubricated friction pairs was evaluated. Friction tests were performed on a ball-on-disc tribometer under lubrication with cutting fluid. The surface texture of the samples before and after the tribological tests was measured using a confocal profilometer. The results obtained from the tests and analysis allow for the conclusion that the use of DLC coatings a-C:H:W increases the hardness of 100Cr6 steel by three times. The values of the contact angles were indicative of surface hydrophilic characteristics. The tungsten-doped diamond-like coating under friction conditions reduced the coefficient of friction and wear. DLC coatings a-C:H:W lubricated with the cutting fluid improve the mechanical and tribological properties of 100Cr6 steel sliding surfaces under friction.



Citation: Radoń-Kobus, K.; Madej, M.; Kowalczyk, J.; Piotrowska, K. Properties of Diamond-like Tungsten-Doped Carbon Coatings Lubricated with Cutting Fluid. *Coatings* **2024**, *14*, 342. <https://doi.org/10.3390/coatings14030342>

Academic Editors: Martin Sahul and Lubomír Čaplovič

Received: 19 February 2024

Revised: 5 March 2024

Accepted: 11 March 2024

Published: 13 March 2024



Copyright: © 2024 by the authors. Licensee MDPI, Basel, Switzerland. This article is an open access article distributed under the terms and conditions of the Creative Commons Attribution (CC BY) license (<https://creativecommons.org/licenses/by/4.0/>).

Keywords: DLC coating; friction; cutting fluid; wear; hardness; SEM

1. Introduction

In order to meet the demands of rapidly advancing technology, it is critical that frictionally interacting components have sufficient tribological, mechanical, and corrosion-resistant properties for enhanced reliability and service life. These properties are strongly dependent on the condition of the surface layer. The properties of the component surface layer are determined by the choice of method and finishing parameters [1–4].

Depending on the intended use of the components, various mechanical treatments are used, such as grinding, sandblasting, polishing, and surface modification by the deposition of coatings [4,5]. The extended life of the components is a constantly evolving topic [6]. Improvements in functional properties are achieved through the use of conventional and unconventional technologies, which include laser and electrical discharge machining, electrochemical and chemical deposition, additive technologies (3D printing) [7], and modern methods of coating deposition by vacuum techniques [8–10], such as CVD and PVD gas-phase deposition [11], often further assisted by plasma [11–13], or ALD atomic layer deposition [14]. The main advantage of these methods is the improvement obtained in the material properties without changing its dimensions. The coating thickness ranges from 100 nm to 5 μm .

In addition to ensuring enhanced friction and wear performance, coatings serve decorative and protective purposes [12,13].

The cutting tool industry has become an essential market for protective coatings. Their important functional characteristics are high hardness, wear resistance, and chemical

inertness. These properties are inherent in diamond-like carbon (DLC) coatings consisting of bonds such as sp^3 , characteristic of diamond; sp^2 , characteristic of graphite; and sp^1 with α and β carbene structures [15–17]. Due to their low friction coefficient, corrosion resistance and biocompatibility, DLC coatings are used in medicine for hip, knee, or shoulder implants, blood pumps, heart valves, or artificial heart components [18–22].

Various types of interlayers and doping with metallic or non-metallic elements are used to improve the adhesion and functional properties of coatings (Figure 1).

Doping DLC coatings improve adhesion, friction-wear, electrical and thermal resistance, biocompatibility, surface energy, and reduced internal stresses [23]. Among the elements most commonly chosen for doping, tungsten enhances tribological properties at elevated temperatures.

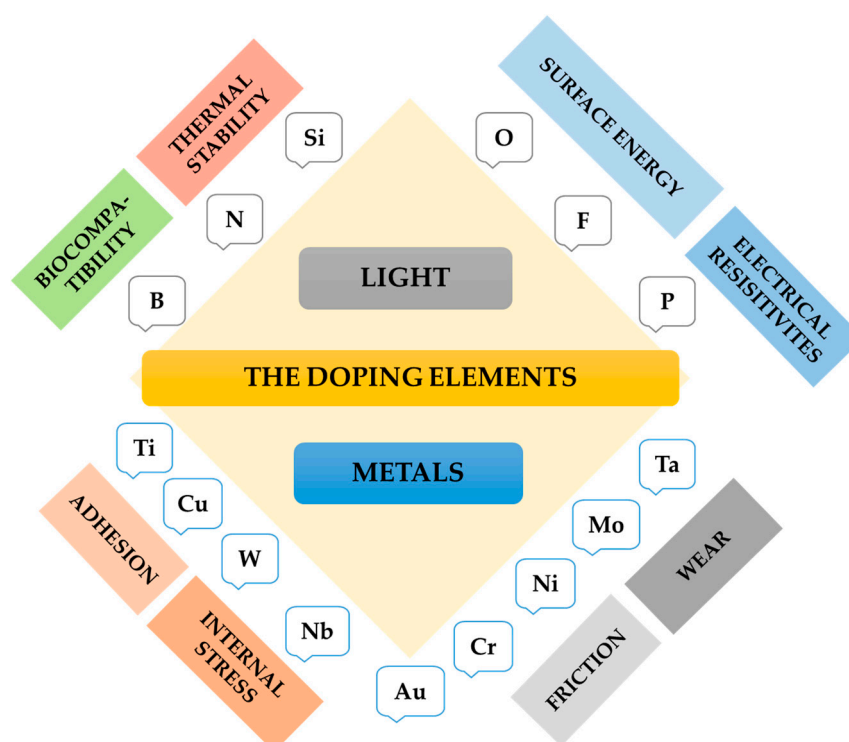


Figure 1. Effects of chemical elements on DLC coatings [24].

Yetim et al. [25] studied the effect of doping a DLC coating with Ti, Al, and V on structural, mechanical, and tribological properties. The sp^3/sp^2 bond ratio increased, as did hardness, due to the formation of hard carbides; moreover, the doping reduced residual stresses and increased adhesion strength, hardness, and tribological wear resistance.

Bai et al. [26] evaluated the mechanical and tribological properties of three types of diamond-like DLC coatings, undoped and doped with Si and W, in friction-wear tests under dry friction in reciprocating motion. They also evaluated the effect of sliding velocity on the adhesion and wear of the coatings. The dominant wear mechanism of Si-DLC coatings was oxidation, which increased with increasing sliding speed. The degree of the graphitization of undoped and W-doped DLC increased with sliding speed, resulting in a lower coefficient of friction and reduced wear rate. The wear rate of W-DLC coatings with an oxidized surface increased considerably at a medium sliding speed. At high sliding speeds, this increase was smaller.

Piotrowska et al. [27] examined a-C:H:Si coating applied to the surface of Ti13Nb13Zr titanium alloy subjected to different treatments. Polished ($R_a = 0.05 \mu\text{m}$) or sandblasted specimens ($R_a = 1.41 \mu\text{m}$) were compared, microscopic observations, thickness, adhesion, wettability, and surface topography were measured, and tribological tests were performed. The tribological tests were conducted in reciprocating motion under dry friction and

lubrication with the cutting fluid. The adhesion of coatings applied to polished surfaces was higher than on sandblasted surfaces. For the a-C:H:Si deposited coating, lower friction coefficient values and linear and volumetric wear values were obtained on the polished specimen compared to the a-C:H:Si coating applied to the sandblasted disc. In addition, the cutting fluid was found to reduce the friction coefficients of the coating applied to the sandblasted specimen compared to the polished specimen without the coating by about 94%. Microscopic observations of wear traces allowed the authors to identify wear mechanisms; in the case of Ti₁₃Nb₁₃Zr, it was tribochemical wear by oxidation, while scratching and micro-scratching dominated in the case of coatings. The authors of [28] presented the results of a study of the tribological properties of diamond-like DLC coatings doped with tungsten deposited on 100Cr6 steel. The hardness of the DLC coating was determined using a microhardness tester. Friction-wear tests were carried out using a ball-on-disc tribometer at loads of 10 N, 25 N, and 50 N under dry friction. The lowest value of the friction coefficient was obtained at a load of 50 N. It was shown that DLC a-C:H:W type prepared by the PVD technique can be used in non-lubricated tribological systems operating under high loads.

Kadam and his team [29] compared the wear of AISI 4140 alloy steel nitrided without a coating and with a WC/C (a-C:H:W) coating applied by physical vapor deposition. They performed friction-wear tests on a pin-on-disc tribotester under dry friction conditions. After nitriding, the WC/C coating on 4140 steel showed significantly less surface wear than the alloy steel without coating. The results were correlated with the properties determined from the tribological and mechanical characterization.

The authors [30] compared the Cr-GLC coating (made of graphite-like carbon doped with chromium) with the Cr-DL coating (made of diamond-like carbon doped with chromium), which they applied to the Al-Si alloy. They performed tribological tests both dry and with base oil lubrication. They observed that the coefficient of friction under lubricated conditions was reduced by 40% compared to dry friction. They concluded that the Cr-DLC coating was characterized by greater anti-wear resistance under dry and lubricated friction conditions than the Cr-GLC coating, by 15% and over 60%, respectively.

Humphrey et al. [28] focused on comparing the impact of DLC coating on the performance of electric vehicle transmissions compared to a standard steel automotive gear set and a polished steel set and improving the performance of electric car transmissions in extra-urban and urban driving. They found lower viscosity for DLC-coated gears compared to steel gears. DLC coatings will save 1.1 km of range in extra-urban driving and 0.9 km in urban driving.

Podgornik [31] investigated the differences in the behavior of the WC/a-C:H:W coating under conditions of technically dry friction and various lubricants. The tests used PAO, diesel, and gasoline as lubricants and were carried out in various combinations: steel/steel, steel/W-DLC, and steel/DLC. He confirmed that DLC coatings achieve better tribological results during technically dry friction or boundary lubrication than with lubrication. The best tribological properties were obtained for the steel/DLC combination. The use of DLC coatings extends the life of the components used five times.

Kržan et al. investigated [32] the influence of the chemical composition of the lubricant on the tribological properties of a tungsten-doped diamond-like coating during oil lubrication in reciprocating motion. They applied a load of 10 N, increasing to a load of 50 N. The tests lasted 1000 s. The lowest value of the friction coefficient was recorded when using rapeseed oil without additives. It was found that the selected additives were not effective enough to maintain the specified anti-wear boundary layer. The surface of the abrasion mark after lubrication with oils with a very low content of impurities was covered with a tungsten-rich tribofilm.

The present study examined a-C:H:W coatings applied by PVD. The results of tribological tests performed at loads of 10 N and 50 N under lubrication with Swisscool 3000 cutting fluid were compared. Surface structure, mechanical properties, and wettability

were also evaluated. There is currently no work reported on the use of Swisscool 3000 in the study of DLC coatings.

2. Materials and Methods

2.1. Materials

Discs with a diameter of 42 mm and a height of 6 mm made of 100Cr6 steel without coating and with a PVD-deposited tungsten-doped diamond-like carbon coating were used in the tests. 100Cr6 steel balls with a diameter of 6 mm were used as counter surfaces. The 100Cr6 steel is a high-carbon steel used for ball and roller bearings. Its chemical composition is compiled in Table 1.

Table 1. Chemical composition of 100Cr6 steel [33].

| 100Cr6, % Content | | | | | | | | |
|-------------------|----------|-----------|-----------|------------|-------|----------|----------|----------|
| Fe | C | Mn | Si | P | S | Cr | Ni | Cu |
| 95.8–96.7 | 0.95–1.1 | 0.25–0.45 | 0.15–0.35 | max. 0.025 | 0.025 | 1.3–1.65 | max. 0.3 | max. 0.3 |

A key element before coating deposition was the substrate surface preparation. The discs were subjected to grinding and polishing with Pace Technologies equipment. The grinding process used abrasive papers with increasing grain gradations ranging from 120 to 2500 μm . The specimens were polished on cloth with the addition of a polishing slurry with a grain gradation of 1 μm . After preparation, the following values of roughness parameters were obtained for the steel specimens: $S_a = 0.04 \mu\text{m}$, $S_q = 0.04 \mu\text{m}$, and $S_z = 1.92 \mu\text{m}$.

The specimens were then cleaned in an ultrasonic cleaner in ethanol. After that, a-C:H:W diamond-like coatings were applied by plasma-assisted physical vapor deposition, using sputtering at a temperature of $<250 \text{ }^\circ\text{C}$. Before applying the DLC coating, a chrome interlayer was applied. Chromium was used to obtain better adhesion of the coating to the substrate. The process involved heating the parts inside a vacuum chamber and then etching them with argon ions to obtain a clean surface free of contaminants. Once the optimal surface properties were obtained, a high negative voltage was applied to the coating material source. This caused an electric discharge and positive argon ions to spray the material. As a result of evaporation, the atomized metal–tungsten in the gas phase was deposited along with the gas containing the non-metallic component of the hard coating, carbon. As a result of the coating deposition, the following roughness parameters were obtained: $S_a = 0.05 \mu\text{m}$, $S_q = 0.09 \mu\text{m}$, and $S_z = 2.54 \mu\text{m}$. The coatings were made at Oerlikon Balzers.

The tribological tests used SWISSCOOL 3000 (Switzerland) water-based mineral oil cutting fluid, the chemical composition of which is shown in Table 2.

Table 2. Parameters of coolant Swisscool 3000 [34].

| Parameter | Value |
|----------------------------------|-----------------------|
| color | light yellow |
| density at 20 $^\circ\text{C}$ | 9.5 g/cm ³ |
| viscosity at 20 $^\circ\text{C}$ | 25 mm ² /s |
| mineral oil content | 13% |

Swisscool 3000 can be used in turning, milling, drilling, and grinding steel, titanium, cast iron, aluminum, and non-ferrous metals. It does not contain chlorine, active sulfur, or secondary amines. In addition, it is free of boron and formaldehyde, making it safe for operators. The product has good wettability, optimal cooling and lubricating properties, good corrosion protection, and biostability [33].

2.2. Research Methodology

The coating morphologies were examined before tribological testing using the JSM-7100F (JEOL, Tokyo, Japan) scanning electron microscope at a magnification of $\times 2000$. This made it possible to determine the changes in morphology and chemical composition of the resulting tungsten-doped diamond-like coating. The results are shown in Section 3.1.

The thickness of the deposited carbon coatings was examined via microscopic observations of cross-sections using scanning electron microscopy (SEM). An accelerating voltage of 15 kV and a magnification of $\times 10,000$ were used. Linear elemental distributions supplemented the study. The test results are shown in Section 3.2.

The hardness of the coating was tested using a Step 6 testing platform equipped with a micro-hardness gauge. A schematic of the test is shown in Figure 2. A Berkovich indenter with an opening angle of 142.5° and a rounding radius of ~ 100 nm was used for the test, with a loading force of 10 mN and a loading speed of 20 mN/min. The test allowed for the determination of the most important mechanical parameters: Young's modulus, penetration depth, and plastic and elastic performance of the tested materials. Plastic work characterizes a material subjected to load when, after the load is removed, it does not return to its original appearance. Elastic work describes the ability of a material to return to its original state after the force is removed. The test results are shown in Section 3.3.

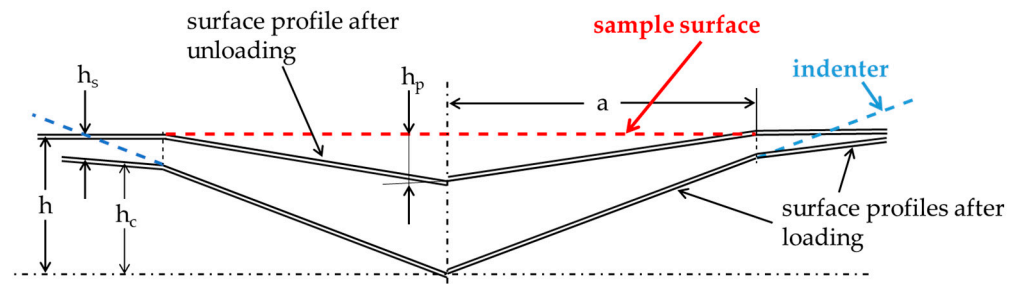


Figure 2. Schematic of the test of instrumental hardness.

The Theta Flex optical tensiometer from Attension was employed to determine the wetting angles of the coating and 100Cr6 steel by the sitting drop method. The wetting angle measurement was carried out by precisely placing a $5 \mu\text{L}$ drop of the measuring liquid (distilled water and Swisscool 3000) on the surface of the specimens and measuring immediately. Figure 3 shows the measurement scheme for the wetting angle value. Five repetitions were performed for each specimen, from which the average wetting angle values were determined. The results of the study are shown in Section 3.4.

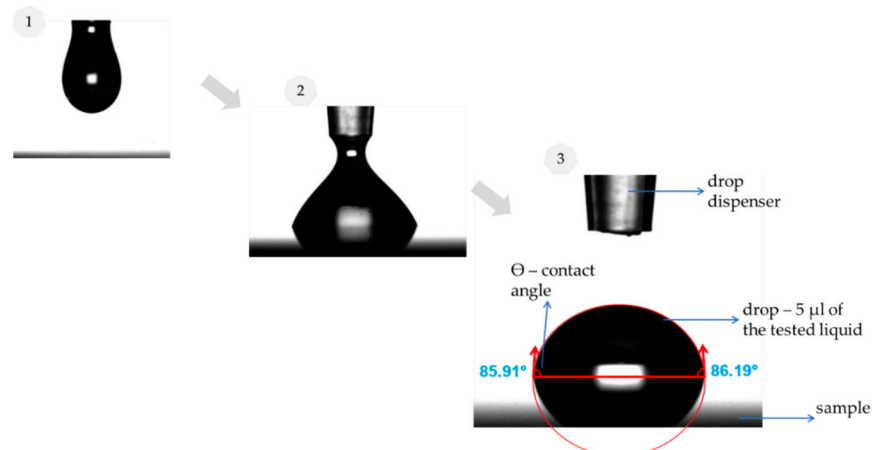


Figure 3. Measurement scheme for the wetting angle value.

Tribological tests were carried out on the Anton Paar TRB³ tribometer in rotating motion, with the parameters under Swisscool 3000 lubrication outlined in Table 3. 100Cr6 steel balls with a diameter of 6 mm were used as counter surfaces. A photograph of the friction pair is shown in Figure 4, while the results of tribological tests are presented in Section 3.5.

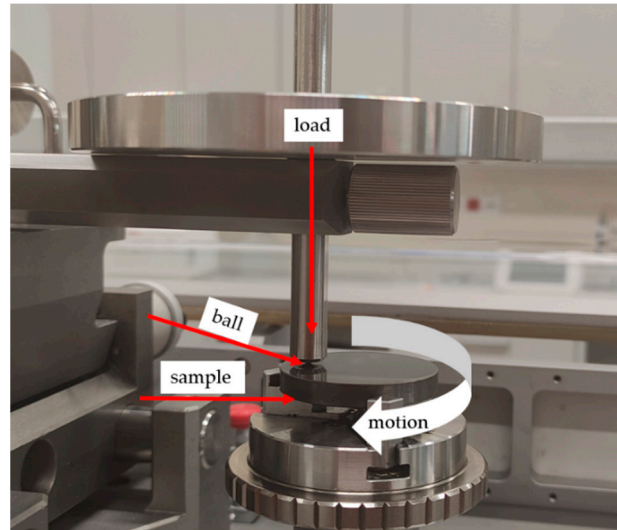


Figure 4. Friction pair.

Table 3. Parameters of tribological test.

| | |
|---------------------|-------------------------------------------|
| Sample—discs | Ø 42 mm—100Cr6 steel with a-C:H:W coating |
| Counter sample—ball | Ø 6 mm—steel 100Cr6 |
| Type of friction | rotation |
| Lubricant | cutting fluid Swisscool 3000 |
| Load | 10 N, 50 N |
| Sliding speed | 0.1 m/s |
| Sliding distance | 1000 m |
| Ambient temperature | 25 ± 1 °C |

The JSM-7100F scanning electron microscope represented the surface morphology of the a-C:H:W coating, 100Cr6 steel, and counter surfaces after friction tests. Observations were carried out at two magnifications: ×300 and ×10,000. The results are presented in Section 3.6.

Using the DCM8 (Leica, Switzerland) confocal mode optical microscope, the geometric structure of the surface after tribological tests was observed. The tests were performed in confocal mode at a magnification of ×20. The area measured was 1.2 mm × 2.3 mm. The results of the tests are presented in Section 3.7.

3. Results

3.1. Surface Morphology

Figure 5a shows an image of the a-C:H:W coating microstructure at a magnification of ×2000 against the X-ray characteristic spectrum, and Figure 5b shows the X-ray characteristic spectrum for tungsten inclusions. Table 4 shows the obtained chemical composition of the tested coating.

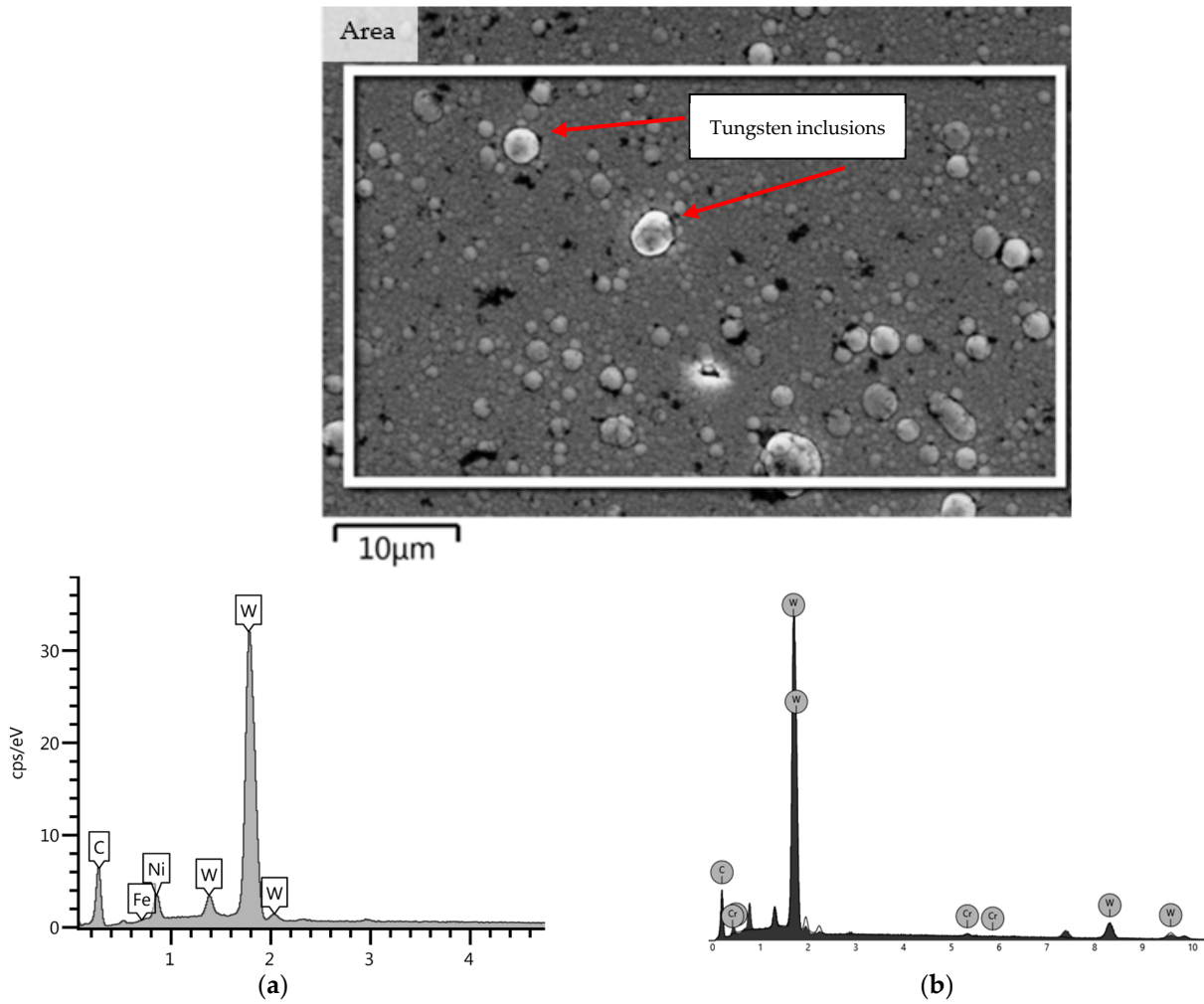


Figure 5. Microstructure of a-C:H:W coating and the X-ray characteristic spectrum: (a) coating (b) and tungsten inclusions.

Table 4. Chemical composition of a-C:H:W coating.

| Spectrum | C | Cr | Fe | Ni | W | Total |
|-----------------|-------|------|------|------|-------|--------|
| Area, % Content | 24.13 | 0.95 | 0.49 | 6.09 | 68.36 | 100.00 |

An example X-ray characteristic spectrum was made by averaging the analysis of three different tungsten inclusions. The a-C:H:W coating obtained by physical vapor deposition (PVD) was characterized by a heterogeneous structure. Microstructure studies indicated the presence of tungsten inclusions on the surface of the a-C:H:W coating in the form of beads ranging from 2 µm to 5 µm in diameter.

3.2. Coating Thickness

Figure 6 shows the linear elemental distribution, and Figure 7 shows the SEM image of the cross-sections along with the thickness measurement. The thickness of the coating was determined from observations in three areas.

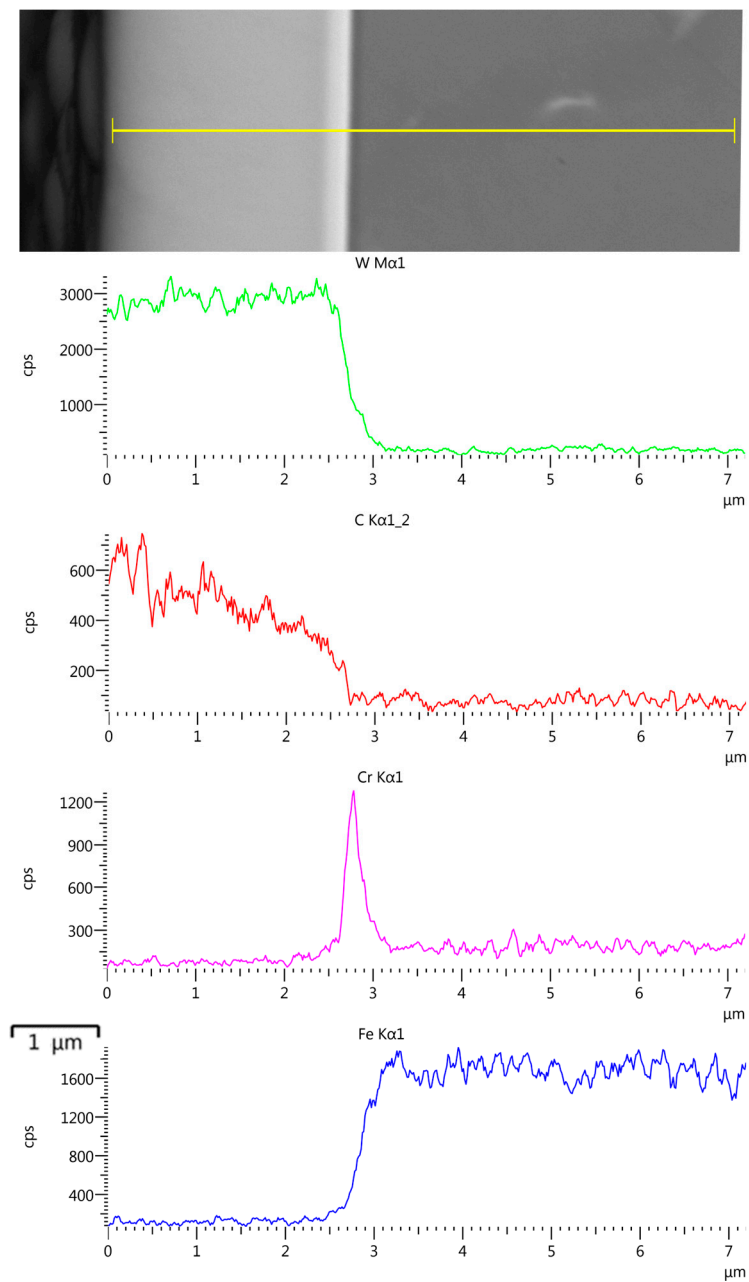


Figure 6. Linear distribution of elements on the cross-section.

Linear analysis of the chemical composition of the a-C:H:W coating showed that the near-surface layer consisted of tungsten and carbon. At a depth of about 2.9 μm from the surface, chromium was observed, constituting the interlayer. It was applied to ensure adequate adhesion of the coating to the metallic substrate. The analysis also indicated the presence of iron from the substrate.

The PVD process resulted in a coating thickness of 3.06 ± 0.1 μm and an interlayer thickness of 0.32–0.48 μm.

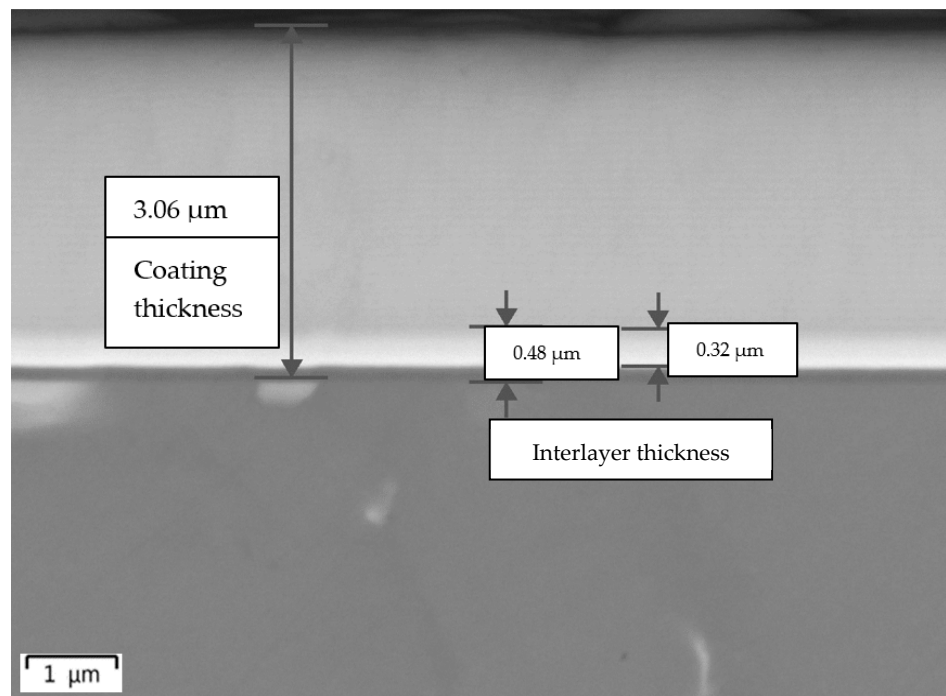


Figure 7. Coating thickness.

3.3. Hardness

Figure 8 presents the load–unload curve as a function of indenter penetration recorded during the hardness test for the reference material and the coating. Table 5 summarizes the most important mechanical parameters of the tested materials.

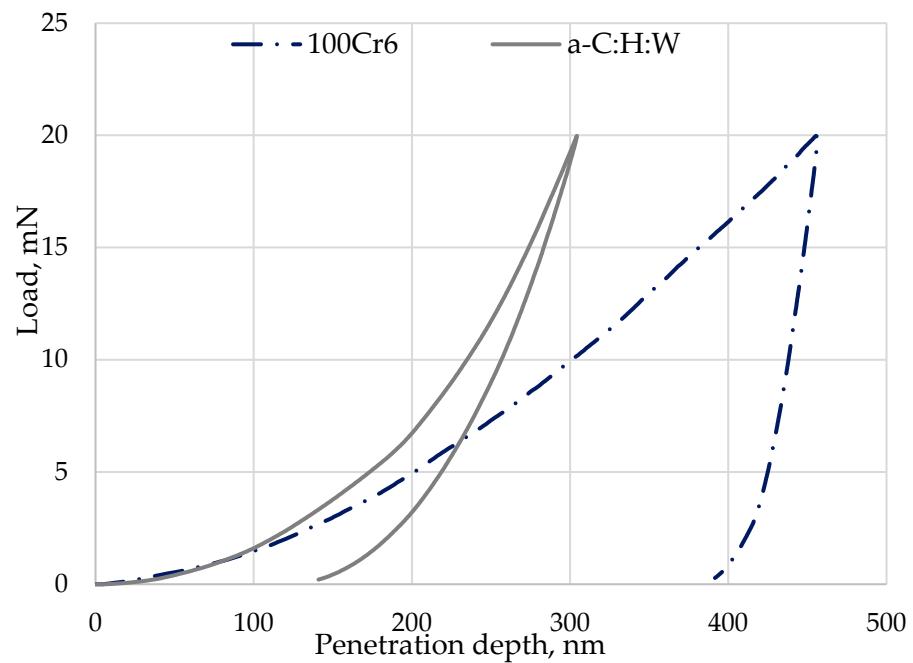


Figure 8. The load–unload curve as a function of indenter penetration recorded during the hardness test for the reference material and the coating.

Table 5. Hardness measurement results.

| Parameter | Mean | |
|---------------------------------------|-------------|--------------|
| | 100Cr6 | a-C:H:W |
| Instrumental hardness— H_{IT} [GPa] | 4 ± 0.1 | 11 ± 1 |
| Young's modulus— E_{IT} [GPa] | 263 ± 5 | 143 ± 26 |
| Maximum penetration depth— h_m [nm] | 457 ± 6 | 318 ± 16 |
| Plastic work— W_{plast} [%] | 89 | 39 |
| Elastic work— W_{elast} [%] | 11 | 61 |

The tests show that the instrumental hardness for the coating was 11.72 GPa, which was almost three-fold higher than for the substrate material. The plastic work for the coating was about 73% lower than for 100Cr6 steel, and the elastic work was about 71% lower for the reference specimen than for the coating.

3.4. Contact Angle

Figure 9 shows sample images of droplets of the measuring fluids, and Figure 10 summarizes the average values of wetting angles for the tested surfaces. Measurements were made with demineralized water and the cutting fluid used during tribological tests.

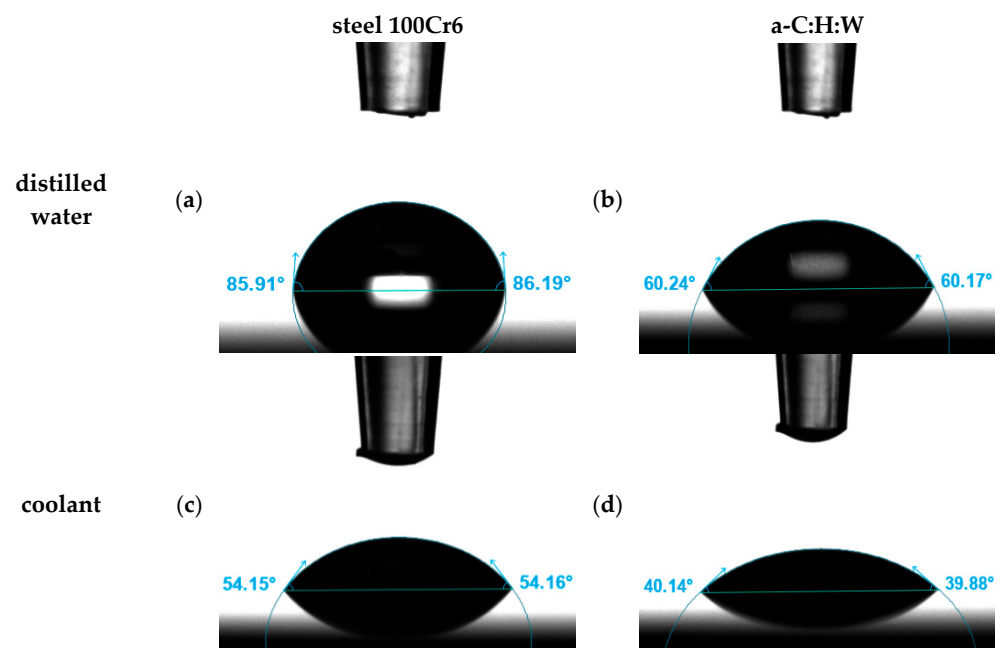


Figure 9. Examples of photographs showing demineralized water droplets (a,b) and coolant (c,d) on steel and a-C:H:W.

The test results indicated that both 100Cr6 steel and a-C:H:W coating had good wettability. This is evidenced by the obtained values of wetting angles below 90° for both test fluids used (demineralized water and cutting fluid). The average value of the wetting angle with demineralized water was about 27% smaller for the coating than for 100Cr6 steel. The a-C:H:W coating wetting angle for the cutting fluid was about 28% smaller than for the reference material.

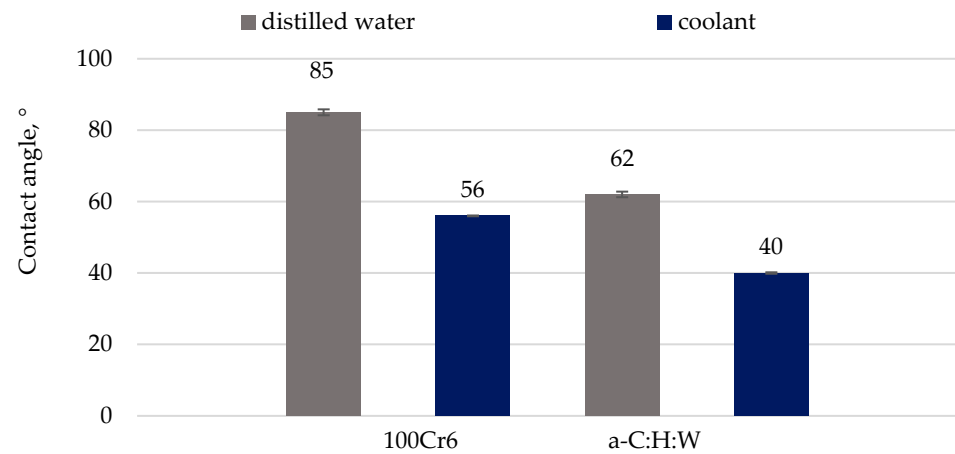


Figure 10. Average values of contact angle.

3.5. Tribological Tests

Figures 11 and 12 illustrate example waveform of friction coefficients and average values of this parameter. Figures 13 and 14 present example waveforms of linear wear and its average values.

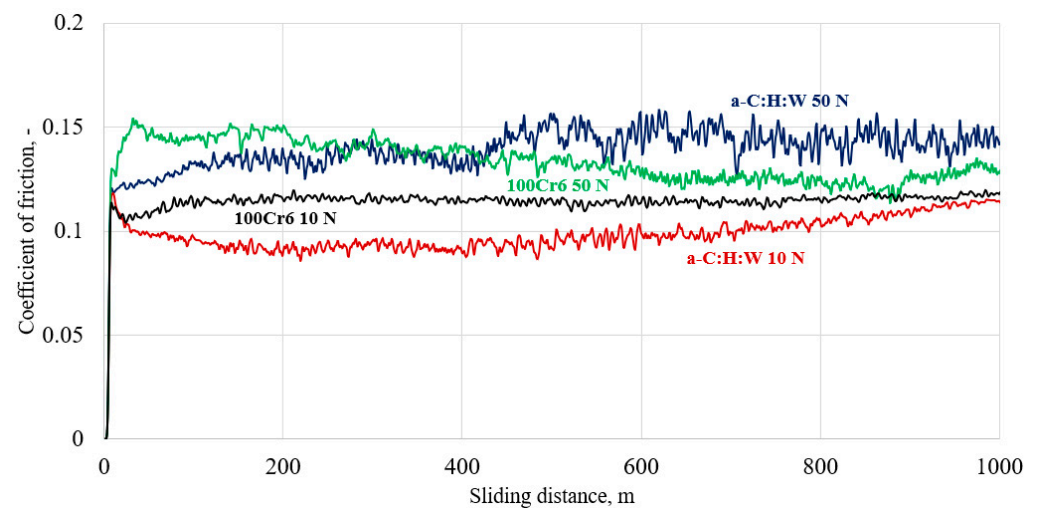


Figure 11. Example waveforms of friction coefficients.

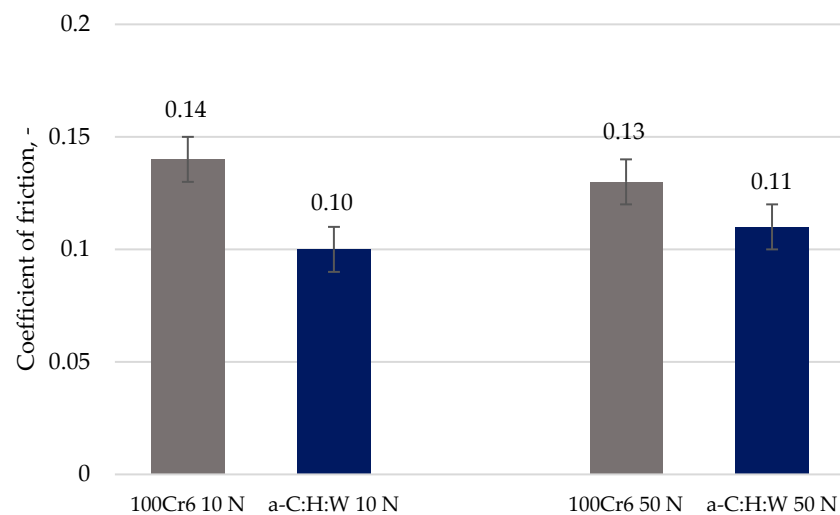


Figure 12. Average values of friction coefficients.

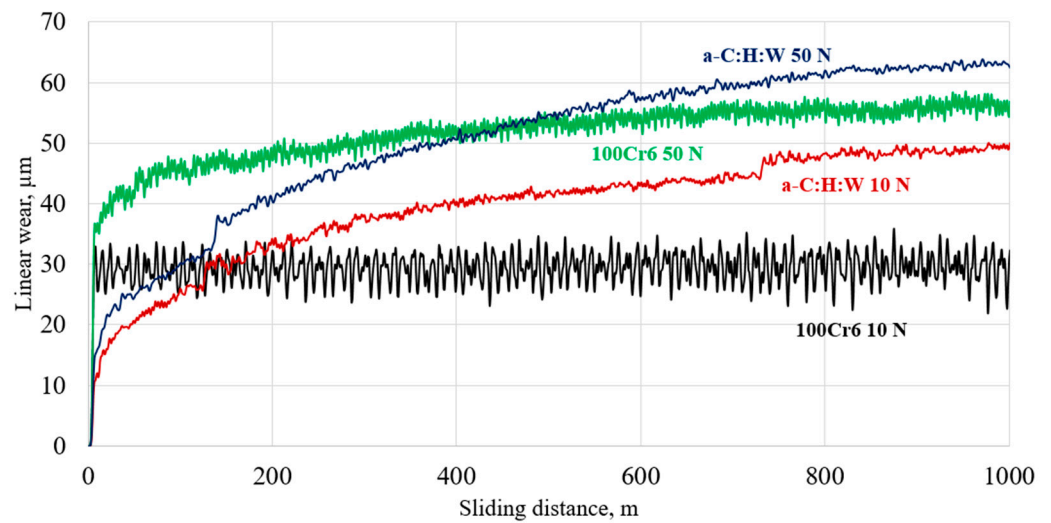


Figure 13. Example waveforms of linear wear.

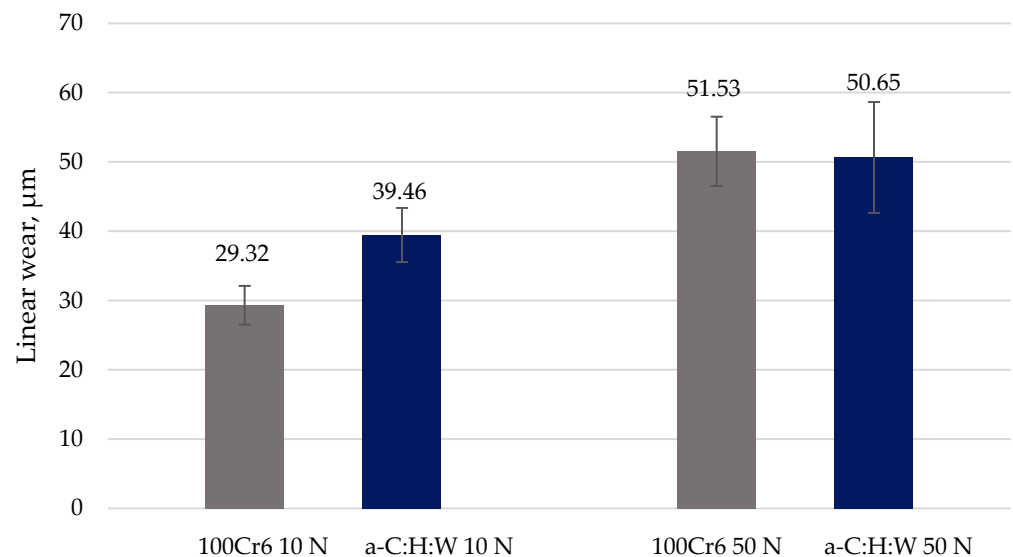


Figure 14. Linear wear average values.

The results of friction-wear tests indicated that 100Cr6 steel exhibited more turbulent friction coefficient plots, both for tests conducted with the 10 N load and 50 N load. In addition, it was observed that for the 10 N load, the coated surface had a lower friction coefficient value of 0.1, which was about 29% lower compared to that of the 100Cr6 steel. For the load of 50 N, the lowest friction coefficient value was obtained for the a-C:H:W coating of 0.11; it was about 15% lower than the value obtained for 100Cr6 steel. It was observed that as the load increased, the coefficient of friction decreased by about 7% for the steel and increased by about 9% for the a-C:H:W coating.

A more stable character of the linear wear changes was observed for the a-C:H:W coating, both at 10 N and 50 N load. After a friction distance of 500 m for a load of 50 N, there was an apparent increase in linear wear for the coating, reaching higher values than 100Cr6 steel. This was most likely due to the more intensive counter surface wear, namely the 100Cr6 steel ball. This required further study using confocal microscopy to determine the wear of the specimens and counter surfaces at the friction nodes analyzed.

When the friction node was loaded with a force of 10 N, approximately 10% lower values of average linear wear were obtained for 100Cr6 steel compared to the a-C:H:W coating. The higher value of the linear wear of the a-C:H:W coating—100Cr6 steel friction node (39.46 µm)—is most likely due to the greater wear of the counter surface, i.e., the ball.

When the friction node was loaded with a force of 50 N, the values were similar but slightly smaller for the coating.

3.6. Evaluation of Surface Morphology after Tribological Tests

Figures 15–22 show SEM images of wear trace morphologies of the specimens and counter specimens after tribological tests. The surfaces were observed at magnifications of $\times 300$ and $\times 10,000$ (areas that were considered characteristic were magnified).

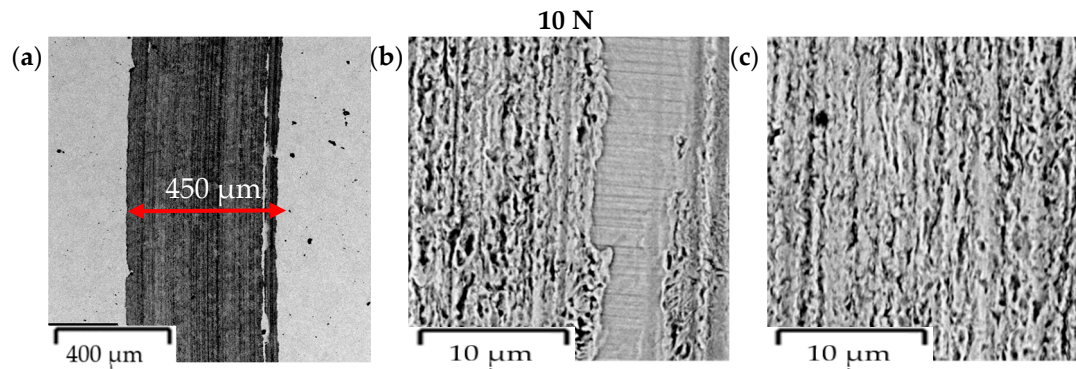


Figure 15. SEM image of disc 100Cr6 steel wear trace: (a) $\times 300$; (b) $\times 10,000$; (c) $\times 10,000$.

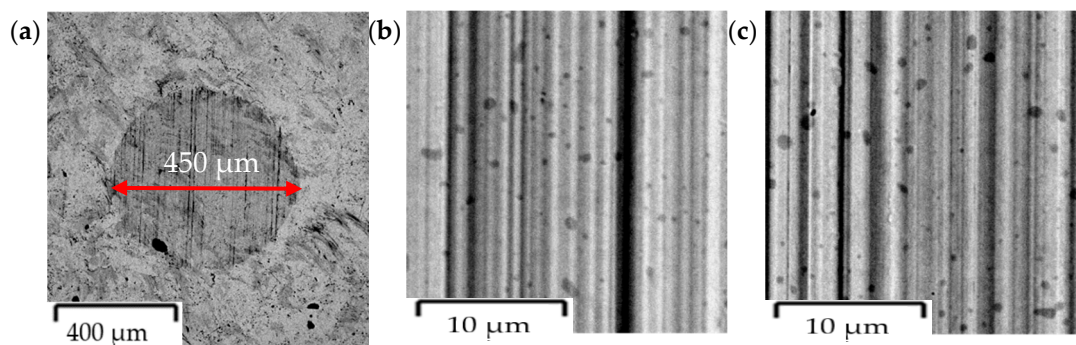


Figure 16. SEM image of the ball wear trace after friction against 100Cr6 steel: (a) $\times 300$; (b) $\times 10,000$; (c) $\times 10,000$.

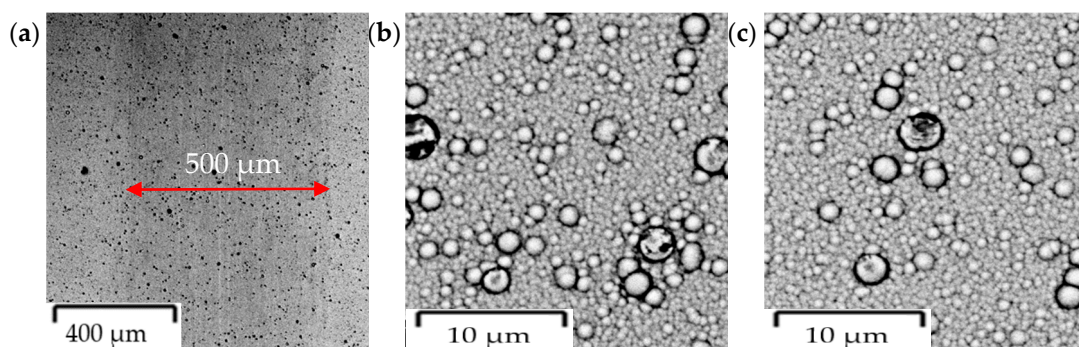


Figure 17. SEM image of disc with coating a-C:H:W wear trace: (a) $\times 300$; (b) $\times 10,000$; (c) $\times 10,000$.

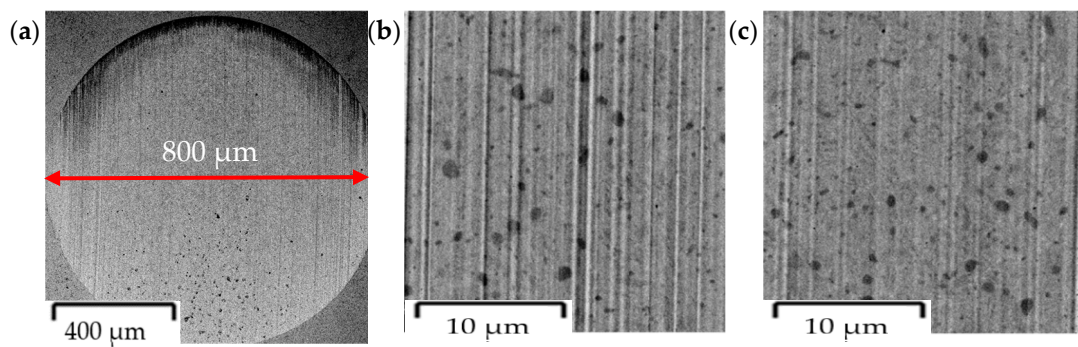


Figure 18. SEM image of the ball wear trace after friction against a-C:H:W coating: (a) $\times 300$; (b) $\times 10,000$; (c) $\times 10,000$.

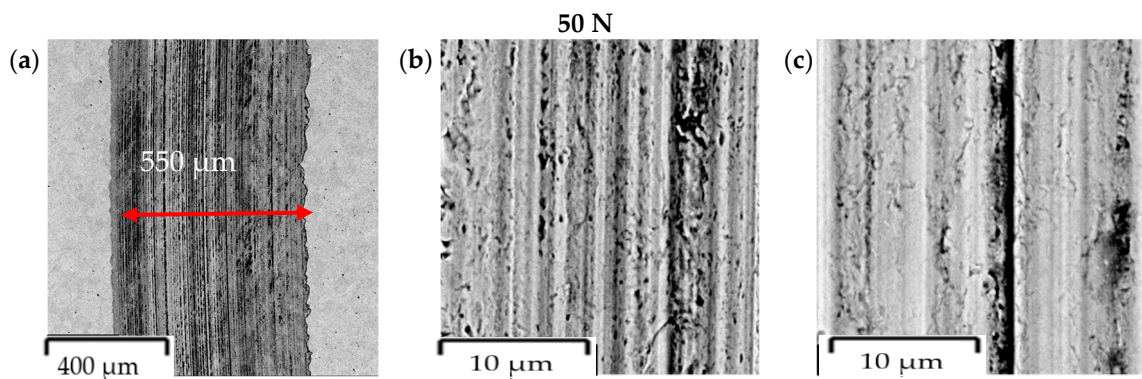


Figure 19. SEM image of disc 100Cr6 steel wear trace: (a) $\times 300$, (b) $\times 10,000$, (c) $\times 10,000$.

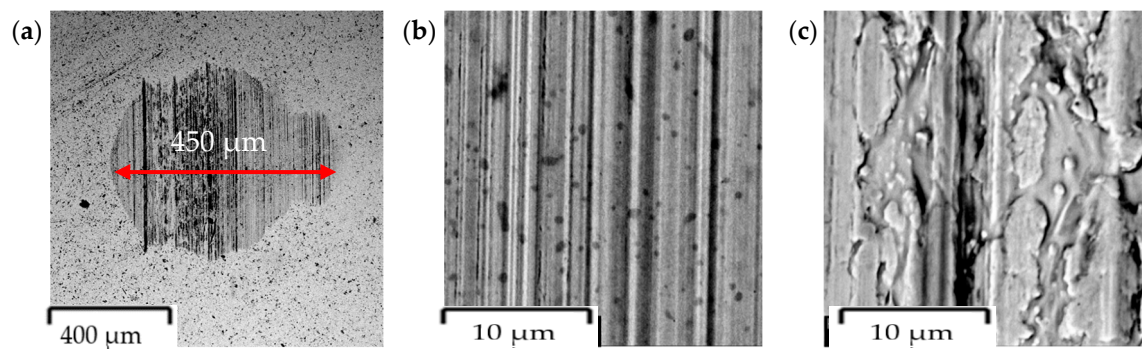


Figure 20. SEM image of the ball wear trace after friction against 100Cr6 steel: (a) $\times 300$, (b) $\times 10,000$, (c) $\times 10,000$.

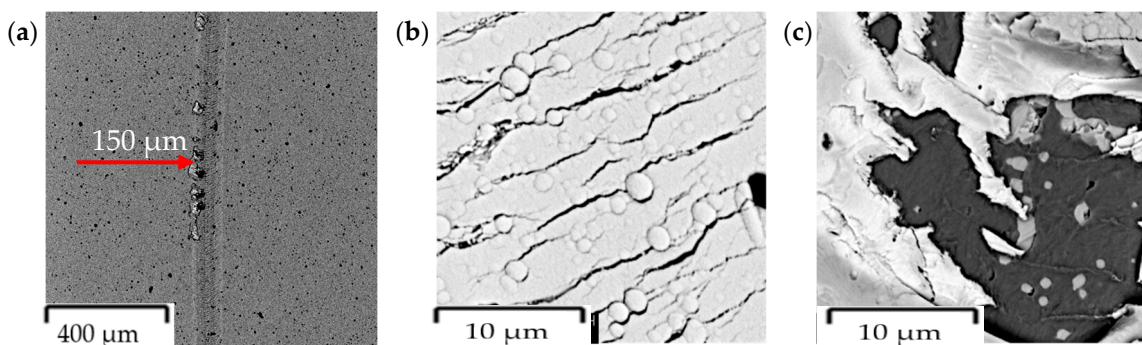


Figure 21. SEM image of disc with coating a-C:H:W wear trace: (a) $\times 300$, (b) $\times 10,000$, (c) $\times 10,000$.

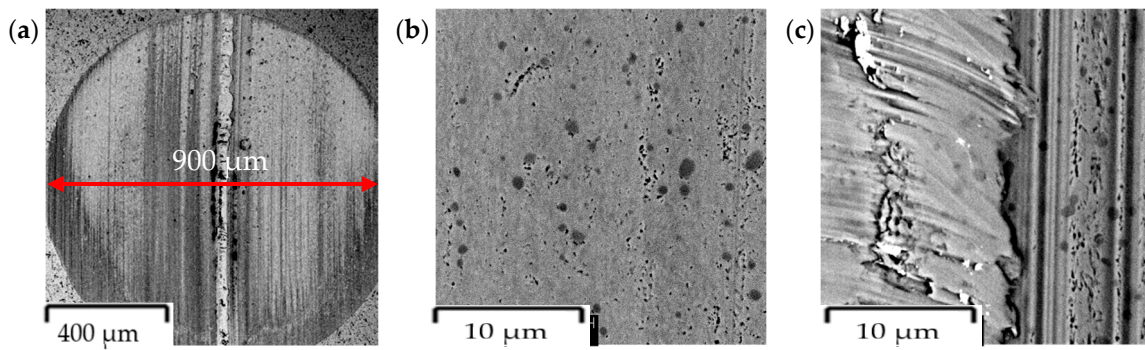


Figure 22. SEM image of the ball wear trace after friction against a-C:H:W coating: (a) $\times 300$, (b) $\times 10,000$, (c) $\times 10,000$.

No wear traces were observed on the a-C:H:W-coated disc under a load of 10 N, while a circular wear trace with a diameter of about 800 μm was measured on the counter specimen. An abrasion trace with a width of 400 μm was found on the 100Cr6 steel and a 450 μm trace on the ball. It was about 44% smaller than that on the ball with the coating after friction.

A 100 μm wear trace was recorded on the a-C:H:W-coated specimen at a load of 50 N, and a 900 μm wear trace was recorded on the counter specimen. Also, traces with a width of 550 μm were observed on 100Cr6 steel. On the ball, it took an irregular shape with a diameter of about 400 μm . It was more than 55% smaller than during friction with the coating. At the same time, the wear trace of the a-C:H:W coating was more than 81% smaller than that for 100Cr6 steel, demonstrating its viability for improving wear resistance. After friction-wear tests, local cracks and chipping were observed on the surface of the coating. Regardless of the applied load in the case of steel discs and balls, the dominant wear mechanism was abrasive wear with furrowing and micro-scratching, and local material transfers.

3.7. Assessment of Surface Geometric Structure of Samples

Figures 23 and 24 show axonometric images and examples of surface profiles after tests with 10 N and 50 N loads. Table 6 summarizes the volumetric wear of the balls after tribological tests for both loads.

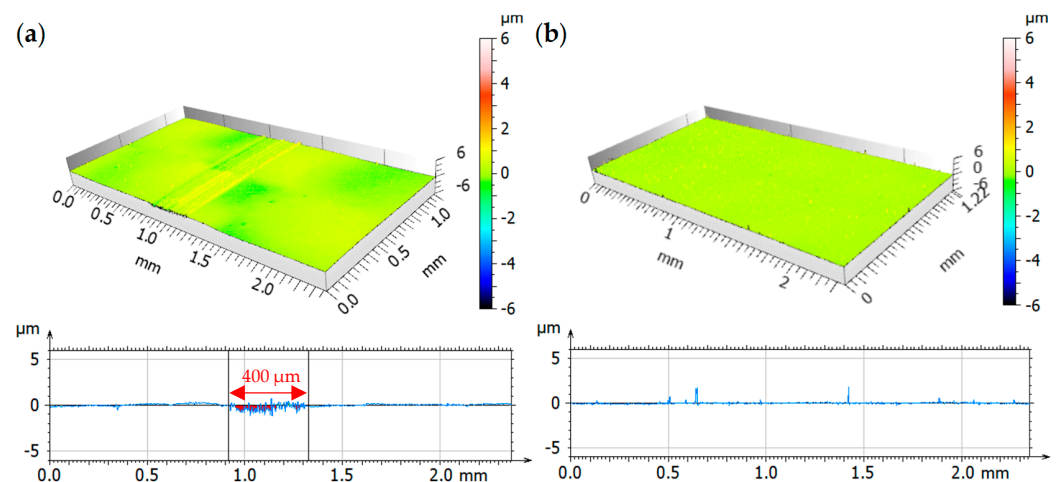


Figure 23. Isometric views and examples of surface profiles after friction tests with a 10 N load for (a) 100Cr6 steel and (b) a-C:H:W coating.

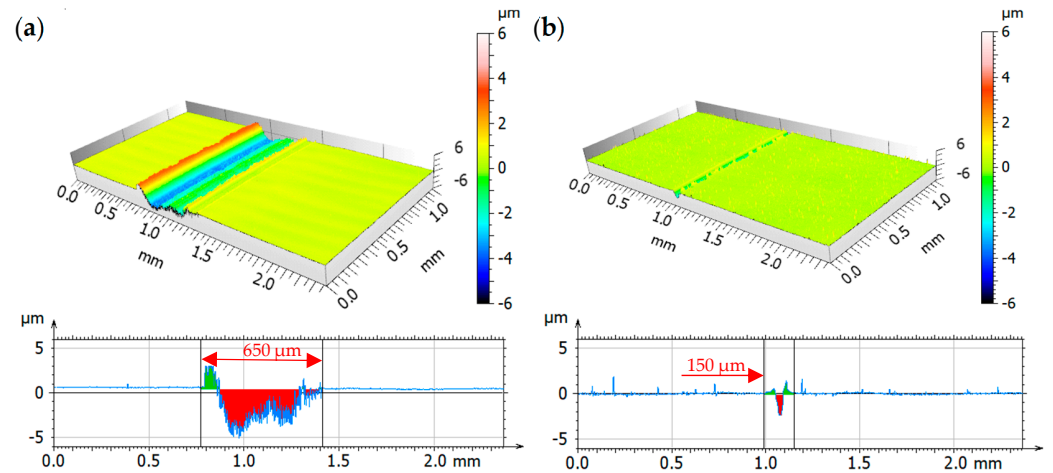


Figure 24. Isometric views and examples of surface profiles after friction tests with a 50 N load for (a) 100Cr6 steel and (b) a-C:H:W coating.

After tribological tests performed at a load of 10 N, no wear trace was observed on the a-C:H:W coating. This proves the high wear resistance of this material. Wear trace with a width of 400 μm and indentations of 1.3 μm were measured on the 100Cr6 steel specimens.

Figures 25 and 26 show optical images of the ball wear traces after tribological tests under 10 N and 50 N loads.

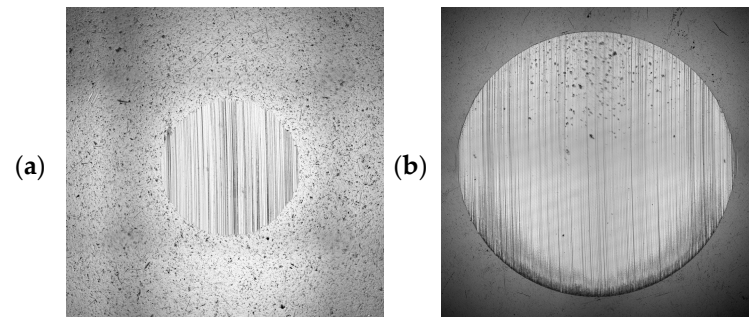


Figure 25. Optical wear images of balls after test with a 10 N load: (a) steel; (b) coating.

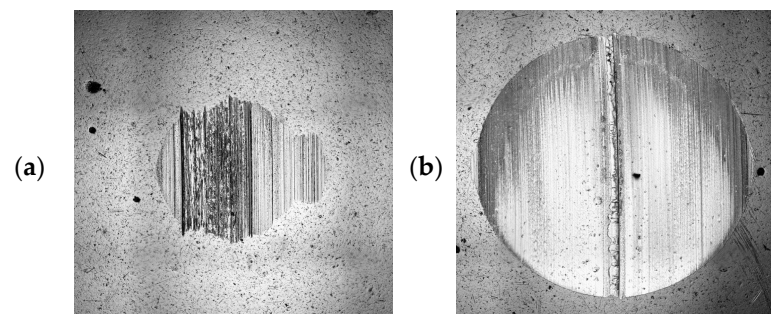


Figure 26. Optical wear images of balls after test with a 50 N load: (a) steel; (b) coating.

At 50 N, the wear trace for 100Cr6 steel was about three-fold wider and deeper compared to the a-C:H:W coating, indicating the higher wear resistance of the tungsten-doped diamond-like coating.

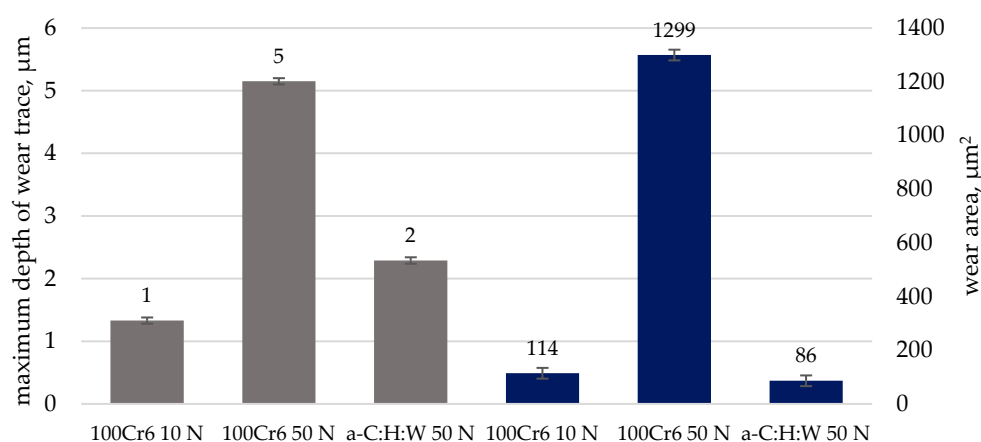
Table 6 shows the volumetric wear of the balls after friction-wear tests.

Table 6. The volumetric wear of the balls after friction-wear tests.

| Ball in Contact with: | Wear Volume, μm^3 | |
|-----------------------|------------------------------|--------------------|
| | 10 N | 50 N |
| steel 100Cr6 | 1.06×10^5 | 7.79×10^5 |
| a-C:H:W coating | 1.22×10^6 | 3.52×10^6 |

The tabulated results show higher ball wear after tests with the a-C:H:W coating. At loads of 10 N and 50 N, the wear of the ball in contact with the uncoated steel disc was 11-fold and 4-fold lower, respectively, than in contact with the coated steel disc.

Figure 27 shows the average values of the wear trace depth and area after tribological tests. Due to the lack of a visible wear trace on the coating at a load of 10 N, it is not included in the graph below.

**Figure 27.** Average value of the wear depth and wear area.

The smallest average value of the wear depth was recorded for the a-C:H:W coating at a load of 50 N. It was about 55% smaller compared to the uncoated steel disc. As for the average wear area values, at the same load, the smallest value was also obtained for the a-C:H:W coating. The average wear trace area for 100Cr6 steel was about 15-fold higher than that of the steel disc with the coating applied to it.

4. Conclusions

The following conclusions were reached based on the findings of this study:

1. The a-C:H:W coating obtained by physical vapor deposition (PVD) was characterized by a heterogeneous structure. Spot analyses of the chemical composition indicated inclusions of tungsten particles. The average thickness of the coating was $3.06 \pm 0.1 \mu\text{m}$.
2. The application of the coating contributed to a 3-fold increase in the hardness of instrumental steel 100Cr6.
3. The results of wetting angle measurements indicated that both tested surfaces were characterized by hydrophilic properties. The smallest values of wetting angles were obtained for the a-C:H:W coating. They were about 27% smaller compared to 100Cr6 steel.
4. Modification of the surface layer by deposition of carbon coatings doped with tungsten contributed to a significant increase in the wear resistance of 100Cr6 steel. In addition, good frictional cooperation was observed between the a-C:H:W coating and the applied cutting fluid.
5. The results of tribological tests carried out with loads of 10 N and 50 N and microscopic observations of wear traces indicated that the a-C:H:W coating was characterized by the smallest coefficients of friction and good anti-wear resistance. The coefficients

were 0.1 and 0.11, respectively, and were smaller by about 20% compared to the values obtained for steel 100Cr6. In addition, no wear traces were observed on a-C:H:W-coated specimens loaded with a force of 10 N; in the case of 50 N, the wear area was more than 15-fold smaller compared to the uncoated steel specimen.

6. The dominant wear mechanism for 100Cr6 steel and the balls was abrasive wear with furrowing and adhesive wear. Micro-scratching and chipping of the deposited coating were observed on the surface of the coating.
7. The application of diamond-like coatings of a-C:H:W type in the friction node studied improved the tribological properties through the use of cutting fluid. A synergistic interaction was observed between the surfaces of the friction pairs analyzed and the cutting fluid used for testing.

Author Contributions: Conceptualization: K.P., M.M., J.K. and K.R.-K.; methodology: K.P. and M.M., writing—original draft preparation: K.P. and K.R.-K.; writing—review and editing: K.P., M.M., J.K. and K.R.-K., supervision, M.M. All authors have read and agreed to the published version of the manuscript.

Funding: This research received no external funding.

Institutional Review Board Statement: Not applicable.

Informed Consent Statement: Not applicable.

Data Availability Statement: Data are contained within the article.

Conflicts of Interest: The authors declare no conflicts of interest.

References

1. Burakowski, T.; Marczak, R. Eksploatacyjna warstwa wierzchnia i jej badanie. *Zagadnienia Eksploat. Masz.* **1995**, *3*, 327–337.
2. Musiał, J. Zmiany zachodzące w warstwie wierzchniej w kolejnych fazach jej istnienia. *Tribologia* **2008**, *3*, 365–374.
3. Niemczewska-Wójcik, M.; Madej, M.; Kowalczyk, J.; Piotrowska, K. A comparative study of the surface topography in dry and wet turning using the confocal and interferometric modes. *Measurement* **2022**, *204*, 112144. [[CrossRef](#)]
4. Náprstková, N.; Novák, M.; Sviantek, J. Specific Cutting Conditions of 100Cr6 Steel Grinding and Selected Final Roughness Parameters. *Adv. Sci. Technol. Res. J.* **2020**, *14*, 184–189. [[CrossRef](#)]
5. Walczak, M. Surface Characteristics and Wear Resistance of 316L Stainless Steel. *Adv. Sci. Technol. Res. J.* **2023**, *17*, 124–132. [[CrossRef](#)]
6. Wolf, V.; Dobrucka, R.; Przekop, R.; Haubold, S. Innovation strategies in the context of the paradigm of the five dimensions of innovation strategy. *Logforum* **2021**, *2*, 205–211. [[CrossRef](#)]
7. Kozior, T.; Hanon, M.M.; Zmarzły, P.; Gogolewski, D.; Rudnik, M.; Szot, W. Evaluation of the Influence of Technological Parameters of Selected 3D Printing Technologies on Tribological Properties. In *3D Printing and Additive Manufacturing*; Ann Liebert, Inc.: New Rochelle, NY, USA, 2023.
8. Vican, M.; Krajánek, D.; Trško, L.; Bokuvka OBuchčík, M.; Florková, Z.; Frkán, M. Improving of 100Cr6 Steel Corrosion and Wear Properties in Simulated Sea Water Environment by Tungsten-Doped DLC Coating. *Materials* **2023**, *16*, 4334. [[CrossRef](#)]
9. Sovelto, O. *Principles of Lasers*; Springer: Berlin/Heidelberg, Germany, 2010.
10. Orman, J.; Radek, N.; Pietraszek, J.; Wojtkowiak, J.; Szczepaniak, M. Laser Treatment of Surfaces for Pool Boiling Heat Transfer Enhancement. *Materials* **2023**, *16*, 1365. [[CrossRef](#)]
11. Milewski, K.; Kudliński, J.; Madej, M.; Ozimina, D. The interaction between diamond like carbon (DLC) coatings and ionic liquids under boundary lubrication conditions. *Metalurgija* **2017**, *1–2*, 55–58.
12. Madej, M.; Marczevska-Boczkowska, K.; Ozimina, D. Effect of tungsten on the durability of diamond-like carbon coatings in the chemical industry. *Przemysł Chem.* **2014**, *93*, 500–505.
13. Madej, M.; Ozimina, D.; Kurzydłowski, K.; Płociński, T.; Wiciński, P.; Styp-Rekowski, M.; Matuszewski, M. Properties of diamond-like carbon coatings deposited on CoCrMo alloys. *Trans. FAMENA* **2015**, *39*, 79–88.
14. Oviroh, P.O.; Akbarzadeh, R.; Pan, D.; Coetzee, R.A.M.; Jen, T.-C. New development of atomic layer deposition processes, methods and applications. *Sci. Technol. Adv. Mater.* **2019**, *20*, 465–496. [[CrossRef](#)]
15. Robertson, J. Diamond like amorphous carbon. *Mater. Sci. Eng.* **2002**, *37*, 129–281. [[CrossRef](#)]
16. Michalczewski, R.; Kalbarczyk, M.; Słomka, Z.; Sowa, S.; Łuszcz, M.; Osuch-Słomka, E.; Maldonado-Cortés, D.; Liu, L.; Antonov, M.; Hussainova, I. The wear of PVD coated elements in oscillation motion at high temperature. *Proc. Estonian Acad. Sci.* **2021**, *70*, 500–507. [[CrossRef](#)]
17. Mozgovoy, S.; Hardell, J.; Prakash, B. High Temperature Friction and Wear Performance of PVD Coatings under Press Hardening Contact Conditions. *Adv. Tribol.* **2019**, *2019*, 4981246. [[CrossRef](#)]

18. Kaneko, M.; Hiratsuka, M.; Alanazi, A.; Nakamori, H.; Namiki, K.; Hirakuri, K. Surface Reformation of Medical Devices with DLC Coating. *Materials* **2021**, *14*, 376. [CrossRef]
19. Sulaiman, M.H.; Farahana, R.N.; Mustafa, M.N.; Bienk, K. Tribological properties of DLC coating under lubricated and dry friction condition. *IOP Conf. Ser. Mater. Sci. Eng.* **2019**, *670*, 012052. [CrossRef]
20. Kržan, B.; Kalin, M.; Jože, J. Tribological behaviour of tungsten-doped DLC coated gears. *Metalurgija* **2008**, *47*, 290–298.
21. Antonowicz, M.; Kurpanik, R.; Walke, W.; Basiaga, M.; Sondor, J.; Paszenda, Z. Selected Physicochemical Properties of Diamond Like Carbon (DLC) Coating on Ti-13Nb-13Zr Alloy Used for Blood Contacting Implants. *Materials* **2020**, *13*, 5077. [CrossRef]
22. Czyżniewski, A. Powłoki DLC w zastosowaniu do pokrywania elementów maszyn. *Inżynieria Mater.* **2003**, *6*, 435–438.
23. Evaristo, M.; Fernandes, F.; Cavaleiro, A. Room and High Temperature Tribological Behaviour of W-DLC Coatings Produced by DCMS and Hybrid DCMS-HiPIMS Configuration. *Coatings* **2020**, *10*, 319. [CrossRef]
24. Sánchez-López, J.C.; Fernández, A. Doping and alloying effects on DLC coatings. In *Tribology of Diamond-like Carbon Films*; Donnet, C., Erdemir, A., Eds.; Springer: Boston, MA, USA, 2008.
25. Yetim, A.; Kovacı, H.; Kasapoğlu, A.; Bozkurt, Y.; Çelik, A. Influences of Ti, Al and V metal doping on the structural, mechanical and tribological properties of DLC films. *Diam. Relat. Mater.* **2021**, *120*, 108639. [CrossRef]
26. Bai, M.; Yang, L.; Li, J.; Luo, L.; Sun, S.; Inkson, B. Mechanical and tribological properties of Si and W doped diamond like carbon (DLC) under dry reciprocating sliding conditions. *Wear* **2021**, *484–485*, 204046. [CrossRef]
27. Piotrowska, K.; Madej, M.; Kowalczyk, J.; Radoń-Kobus, K. Surface Roughness Effects on the Properties of Silicon-Doped Diamond-like Carbon Coatings. *Coatings* **2023**, *13*, 1629. [CrossRef]
28. Humphrey, E.; Elisaus, V.; Rahmani, R.; Mohammadpour, M.; Theodossiadis, S.; Morris, N. Diamond like-carbon coatings for electric vehicle transmission efficiency. *Tribol. Int.* **2023**, *189*, 108916. [CrossRef]
29. Kadam, N.R.; Karthikeyan, G. Wear Evaluation of AISI 4140 Alloy Steel with WC/C Lamellar Coatings Sliding Against EN 8 Using Taguchi Method. *J. Inst. Eng. (India) Ser. C* **2016**, *97*, 547–550. [CrossRef]
30. Al-Samarai, R.A.; Al-Douri, Y. Tribological properties of DLC and GLC coating for automotive engine components application under lubrication. *Int. J. Appl. Mech. Eng.* **2023**, *28*, 10–25. [CrossRef] [PubMed]
31. Podgornik, B. Tribological behavior of DLC films in various lubrication regimes. In *Tribology of Diamond-like Carbon Films*; Springer: Berlin/Heidelberg, Germany, 2009; pp. 410–453.
32. Kržan, B.; Novotny-Farkas, F.; Vižintin, J. Tribological behavior of tungsten-doped DLC coating under oil lubrication. *Tribol. Int.* **2009**, *42*, 229–235. [CrossRef]
33. 100CR6, W.NR 1.3505, EN ISO 683-17 Wysokowęglowa stal Łożyskowa. Available online: <https://steeltrans.com.pl/stale-stopowe/10-stale-lozyskowe/51-100cr6-lh15-wnr-13505-en-iso-683-17> (accessed on 28 July 2023).
34. Technical Data Sheet SWISSCOOL 3000. Available online: https://www.etlfluidexperts.com/Files/Datasheet/MOTOREX/ETL_Fluid_Experts_SWISSCOOL_3000_EN.pdf (accessed on 28 July 2023).

Disclaimer/Publisher’s Note: The statements, opinions and data contained in all publications are solely those of the individual author(s) and contributor(s) and not of MDPI and/or the editor(s). MDPI and/or the editor(s) disclaim responsibility for any injury to people or property resulting from any ideas, methods, instructions or products referred to in the content.